

EBM Technique Study on Microstructural Characterization of Al-Zr-N Coating

R Hariharan¹, Antony Micheal Raj D², M Dharan³, Mohammad Rizal⁴, Jose Robert⁵, V Balambica⁶

^{1,6}Department of Mechanical Engineering, Bharath Institute of Higher Education and Research, Chennai-73, Tamilnadu, India

^{2,3,4,5}Students, Department of Mechanical Engineering, Bharath Institute of Higher Education and Research, Chennai-73, Tamilnadu, India

¹Corresponding Mail ID: hariharan.mech@bharathuniv.ac.in

Abstract

Through the implementation of the electron beam physical vapour deposition (EB-PVD) technique, an aluminium zirconium nitrate (Al-Zr-N) coating has been created in the current work on high speed steel (E19) substrates. Through the use of X-ray diffraction (XRD), scanning electron microscopy (SEM), atomic force microscopy (AFM), nano indentation, and scratch tests, the structural morphological and mechanical properties of the substrate are investigated. The cause of tension relaxation and vacancy concentration is explained by the fluorite phase's lattice constant decreasing with rising deposition temperature. As the temperature of the substrate rises, the coating's increased surface roughness is explained by an increase in crystallite size [1]. TBCs are frequently applied to metal substrates using the Atmospheric Plasma Spraying (APS) and Electron Beam Physical Vapour Deposition (EB-PVD) methods. For the next generation of turbine engines, the high costs and relatively high thermal conductivities of EB-PVD coatings, as well as the short thermal lifetime of APS coatings, are significant drawbacks. Suspension Plasma Spraying (SPS) was evaluated in this study to enhance the thermal properties of TBC. The SPS process enables the creation of columnar micro-structures that are easily adjustable in terms of thermal conductivity and columnar structure compaction.

Keywords: EB-PVD coatings, Atmospheric Plasma Spraying (APS), X-ray diffraction (XRD), scanning electron microscopy (SEM), atomic force microscopy (AFM)

I. Introduction

Because air plasma in spraying (APS) and electron beam physical vapour deposition (EB-PVD) are the two primary methods used to deposit thermal barrier coatings (TBCs), EB-PVD is a better option for coating substrates because it has a smoother surface, a stronger bond, and better strain tolerance. A focused high energy electron beam is used in the high vacuum thermal coating technique known as electron beam physical vapour deposition (EB-PVD) to melt an evaporant material inside of a vacuumed chamber. This method is thought to be straightforward and reasonably inexpensive. TBCs are defence mechanisms that encourage more effective gas turbine engines and increased metallic component lifetime. The evaporating substance is then concentrated on a substrate's surface.

Among those factors that has the greatest impact on the microstructure and longevity of the coatings is substrate temperature. Therefore, research into Al-Zr-structural N's and mechanical characteristics is necessary. In order to understand how the substrate temperature affects the growth characteristics of the Al-Zr-N coatings, the Al-Zr-N properties of the electron beam evaporated Al-Zr-N coatings at different substrate temperatures have been examined in this study. The superalloy's composition and its interactions with the BC, particularly in EB-PVD TBC devices, have a significant impact on TBC lifetime.

In order to raise gas turbine engine operating temperatures and increase efficiency, the aviation industry is working to create Thermal Barrier Coatings (TBCS) that are more effective at shielding metallic alloys. Enhancing the insulating capability of TBC ceramic layers is a crucial goal. For the next generation of gas turbine engines, novel coatings and processing techniques are being developed due to the low cost of the EB-PVD process [2-4].

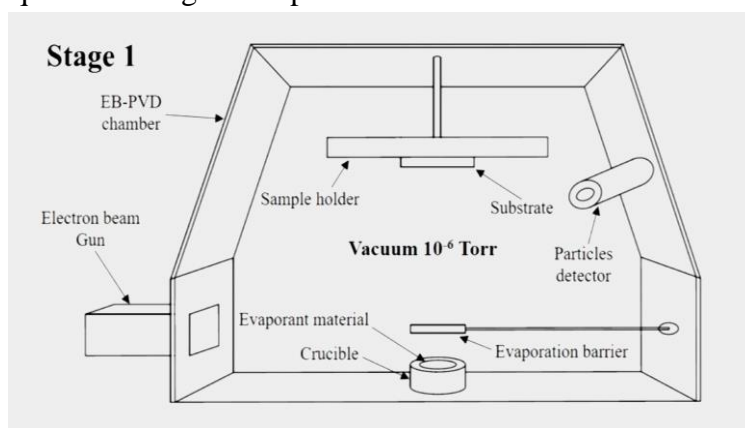


Fig.1 schematic illustration of the device configuration [4]

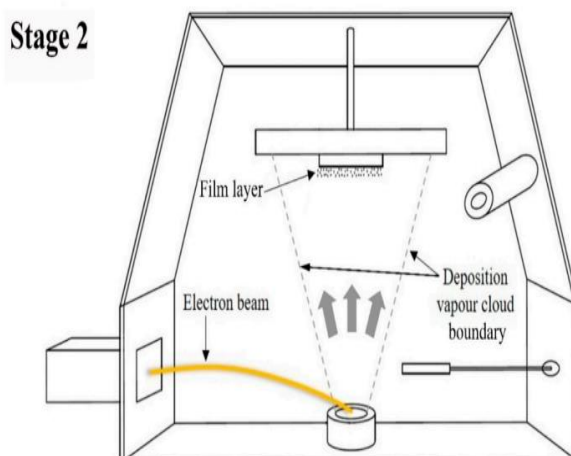


Fig.2 Evaporation and film formation [4]

II. Experiment

The process variables, particularly the substrate temperature, chamber pressure, and deposition rate, completely determine the crystal structure and shape of EB-PVD. Alumina substrates of 1 mm thickness were used as the base material to deposit Al-Zr-N in order to prevent harm to metallic substrates, such as nickel-based super alloys and bond coats, during the high temperature infiltration experiments for an extended period of time.

Using an energy dispersive spectrometer (EDS) and a scanning electron microscopy (SEM) attached to an EDAX detector, the microstructural changes were examined from

polished cross-sections (EDS). The structural alterations of the ceramic coatings on the surface and in the cross-section were monitored using Raman micro-spectrometry and X-ray diffraction (XRD) in the 0-20 mode with Cu radiation, respectively.

The peak intensities of slow scans (step size of 0.01° at a dwell time of 10 s per step) on the ranges of interest— $2\theta = 27$ to 32° for the (111) and (111) peaks of the monoclinic phase and $2\theta = 72$ to 76° for the (400) and (004) peaks of the cubic and tetragonal phases—were used to calculate the weight fractions of the tetragonal, monoclinic, and cubic phases. The substrate temperature was set to approximately $900 \pm 50^\circ\text{C}$, and the substrate was moved at a speed of 20 rpm during the EB-PVD process of depositing the Al-Zr-N coating. The covering is roughly 60 to 70 nm thick in each case. [5]

III. Results and Discussion

X-ray diffraction (XRD) patterns were acquired for the substrate and thin films grown at various deposition and post-deposition temperatures using a Rigaku Dmax 2500PC instrument (with Cu K α radiation). The films were produced for 30 minutes before the X-ray diffraction. The peaks corresponding to angles (200), (220), and (311) for the as-grown films (F1 and F5) were less intense than those for the annealed films. The peaks for the films annealed at 550°C were less intense, whereas the high intensities seen for the films annealed at 400°C (with and without O $_2$ flow) demonstrated enhanced crystallisation and larger grain size. The O $_2$ flow's impact on the (200) reflections was disclosed by the XRD results. Peak splitting at roughly 45° (200)/(002) was plainly seen, indicating that the thin films were stabilised in the tetragonal phase, though the splitting could also have been brought on by film strain.

Both the residual strain and the coherent crystal size were determined from the XRD data using a Williamson-Hall analysis. The image obtained showed that both deposition times resulted in much greater compressive strain for the thin films under the higher temperature thermal treatment, though the films deposition during the first 30 minutes had slightly larger grains than the films deposition during the second 45 minutes.

Additionally, the findings demonstrated that the residual compressive strain in the film was highest for films with the best oxygenation and reduced with oxygen deficiency. Understanding the optical characteristics of these films requires a knowledge of the temperature dependence of the residual strain and crystallite size. The AFM measurements indicated that the surface morphology should have a negligible impact on loss of reflection, suggesting the material's potential for use in the creation of photonic components. The thin films in both situations displayed a uniform surface morphology with apparent size grain distributions and surface roughness that were temperature-dependent [6].

EB-PVD characterization and phase transition

As coated EB-PVD coatings were amorphous in nature with a little contribution from cubic gamma phase. It is known from the literature that the phase transition from amorphous to crystalline α -alumina occurs in the temperature range of 900°C - 1200°C . In situ high temperature XRD analysis was performed on the alumina layers and the corresponding phase changes are shown in Fig. 3. Changes in α -alumina peak intensities were very low in the temperature range between 900 - 1050°C and high intensity sharp peaks were

only observed at 1100 °C for 30 min. No meta-stable phases were found in the XRD patterns. Thus, this temperature was taken for further heat of as-coated samples to obtain thermodynamically stable α -alumina topcoats . During the pre-heat treatment heavy sintering of the alumina coating was observed. SEM surface and cross-sectional micrographs ,show the drastic change in microstructure before and after heat treatment. As-coated samples at room temperature have a fully dense coating with very thin inter-columnar gaps . After the heat treatment, shrinkage cracks have appeared. In the cross-sectional analysis these cracks are clearly visible . In addition, a slight change in the intra columnar microstructure was also observed after the crystallization treatment . Alumina columns were found to be more porous after pre-heating than after as coated which is assumed to be due to the crystallization of amorphous alumina. The columns were also found to be shrunk after the heat treatment. The interface adhesion was found to be unaffected by the heat treatment . No cracks or delamination were observed at the in- terface and the adhesion between zirconium layer and aluminium was found to be un-effected by the sintering process.

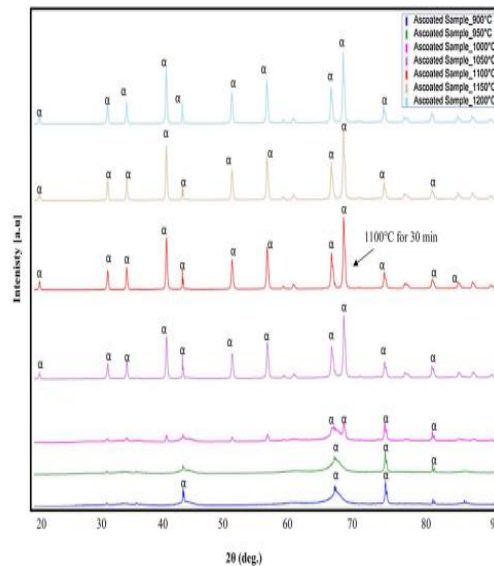


Fig.3 SEM surface and cross-sectional micrographs ,show the drastic change in microstructure before and after heat treatment

EB-PVD 7Y5Z covering on an alumina substrate, in-situ high temperature XRD patterns for coated alumina as-coated. To indicate that all samples were heated at 1100 °C and the coating is entirely crystalline, 1100 °C peaks are only marked with an arrow.

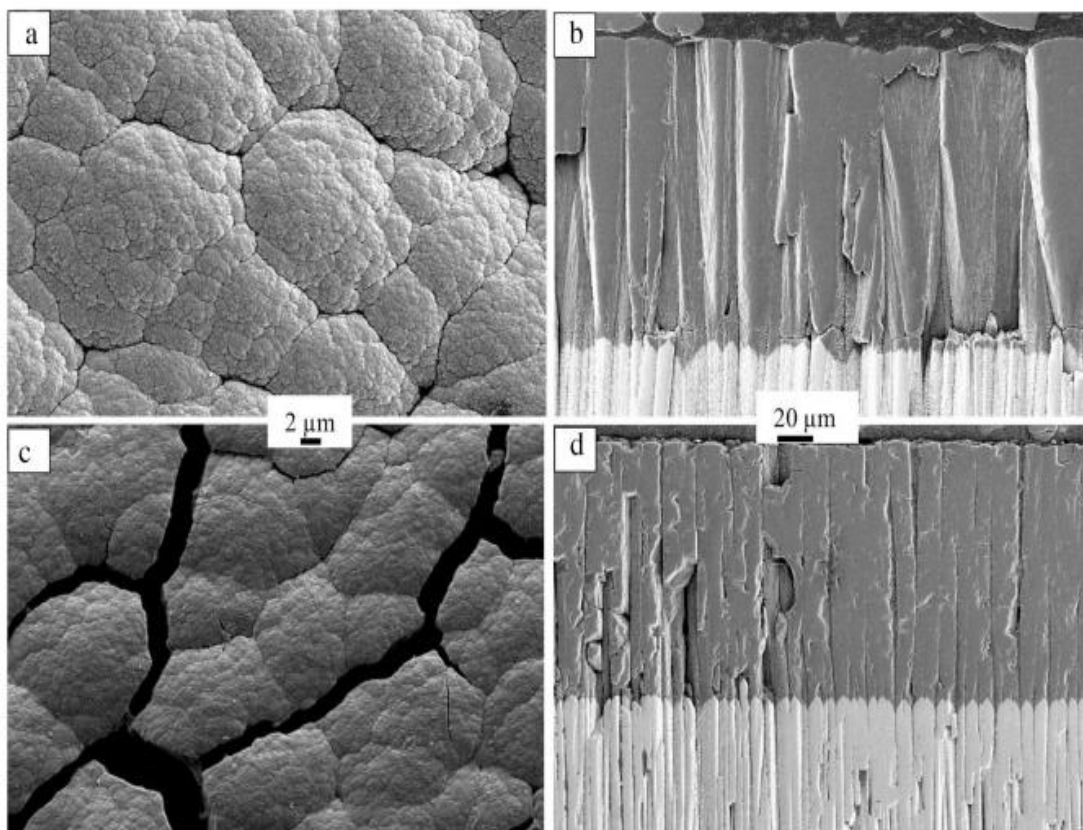


Fig.4 SEM micrographs taken on the top surface of the EB-PVD alumina coating, before (a) and after (c) the heat treatment at 1100 °C for 30 min, (b) and (d) are the cross-sectional images of the Al₂O₃ coating after heat treatment.

In (d) an area of a shrinkage cracks is shown while (b) represents a non-crack region showing a dense alumina coating. Alumina coatings at 1250 °C. The overall SEM cross-sectional view and the Ca element mapping for all the CMAS/VA in- filtrated samples. In all the cases especially in larger cracks, CMAS/VA has reached the 7YSZ interface but no reaction with 7YSZ was observed. It is clear that these larger gaps offer no resistance to the in- filtration but the time was too short for the yttria dissolution in the melt. Shows the high magnification image of the reaction zone, between CMAS 1 and alumina. Based on compositions measured by EDS and the XRD powder mixture results "most likely" formed crystal phases have been identified. The reaction layer which partially seals the inter-columnar gaps was identified as spinel (Sp). Another CMAS crystallizing product on top of spinel was identified as an orthite (An). The light gray contrasted product at the top of the image and at the center of the columnar gaps represents the residual CMAS glass [7].

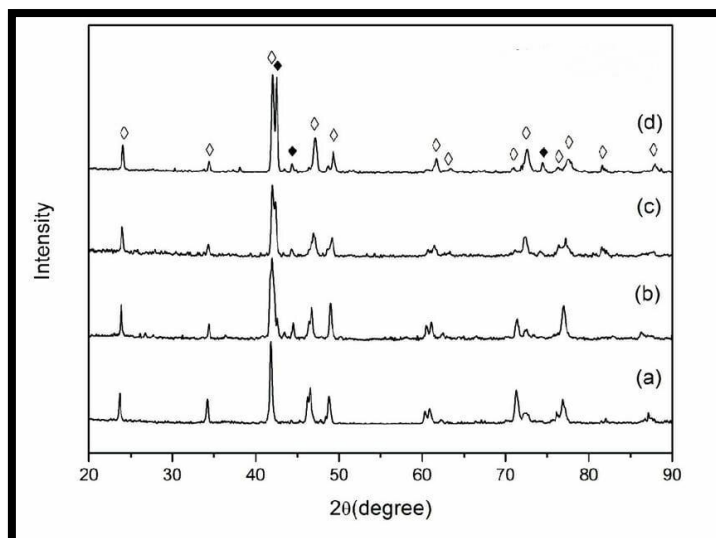


Fig.5 XRD patterns of alumina mixtures

The EB-PVD alumina exhibits a high reactivity with Al-Zr-N and rapidly forms resting products. However, sinter cracks that had been developed during the pre-heat treatment have allowed the Al-Zr-N to locally fully infiltrate. To overcome the microstructural shrinkage effects, a further alumina layer was applied by means of the RBAO method. Alpha- Al_2O_3 was created during the application process itself because of the heat treatment at 1300 °C. Fig. 5 shows the 20-25 μm thick RBAO layer on top of EB-PVD alumina. The microstructure with no macroscopic crack formation or RBAO coating- alumina topcoat debonding was obtained during the process.

IV. Conclusion

Al-Zr-N TBCs were deposited on high speed steel E19 using the EB-PVD method in the current research. TBCs were subjected to hot corrosion experiments at 1000 °C and isothermal oxidation tests at 1000 °C for 8, 24, 50, and 100 hours, respectively. Following the experiments, the following analyses were conducted using XRD, EDS, and mapping:

Both TBC systems showed no signs of delamination or phase transformation after the oxidation experiments.

It was also discovered that the Al content affected the Al-Zr-N thin films' microstructure and crystallinity. Al-Zr-N thin films' crystallinity declined as Al content rose. Additionally, when the Al concentration in Al-Zr-N thin films was 15.9 and 22.2 at.%, Arrhenius graphs displayed nonlinear dependences. The activation energies were 1.10 eV between 400 and 560 °C and 1.85 eV between 720 and 1000 °C. The dissociation of vacancy-dopant cation dimers or trimers, which are oxygen vacancy complexes, could be the cause of the rise in activation energy and conductivity. The Al-Zr-N thin films having 3.8 at.% of AL had the highest total ionic conductivity (bulk =2.89 Sm^{-1} at 800 °C).

Reference

[1] S. Anandh Jesuraj, P. Kuppasami, T. Dharini, Padmalochan Panda Effect of Substrate Temperature on Microstructure and Nanomechanical Properties of $\text{Gd}_2\text{Zr}_2\text{O}_7$ Coatings Prepared by EB-PVD Technique (2018) <https://doi.org/10.1016/j.ceramint.2018.07.024>

- [2] Benjamin Bernard a,d , Aurélie Quet a, Luc Bianchi b, Aurélien Joulia b, André Malié c, Thermal insulation properties of YSZ coatings: Suspension Plasma Spraying (SPS) versus Electron Beam Physical Vapor Deposition (EB-PVD) and Atmospheric Plasma Spraying (APS), (2016) <http://dx.doi.org/10.1016/j.surfcoat.2016.06.010>
- [3] Naser Ali , Joao A. Teixeira , Abdulmajid Addali , Maryam Saeed, Deposition of Stainless Steel Thin Films: An Electron Beam Physical Vapour Deposition Approach,2019, <https://doi.org/10.3390/ma12040571>
- [4] G. Boissonnet, C. Chalk, J.R. Nicholls", G. Bonnet", F. Pedraza, Phase stability and thermal insulation of YSZ and erbia-yttria co-doped zirconia EB-PVD thermal barrier coating systems,2020, <https://doi.org/10.1016/j.surfcoat.2020.125566>
- [5] J. Muñoz Saldaña,b,*,1 , U. Schulza , G.C. Mondragón Rodríguez, Microstructure and lifetime of Hf or Zr doped sputtered NiAlCr bond coat/ 7YSZ EB-PVD TBC systems,2017, <https://doi.org/10.1016/j.surfcoat.2017.12.017>
- [6] Zaoyu Shen, Limin He* , Zhenhua Xu, Rende Mu, Morphological evolution and failure of LZC/YSZ DCL TBCs by electron beam-physical vapor deposition,2018, <https://doi.org/10.1016/j.mtla.2018.10.011>
- [7] J.L. Clabel H.a,* , V.A.G. Riverab , I.C. Nogueirac , E.R. Leited, Effects of defects, grain size, and thickness on the optical properties of BaTiO₃ thin films,2017, <https://doi.org/10.1016/j.jlumin.2017.08.043>
- [8] R. Naraparaju* , R.P. Pubbysetty, P. Mechnich, EB-PVD alumina (Al₂O₃) as a top coat on 7YSZ TBCs against CMAS/VA infiltration: Deposition and reaction mechanisms,2018, <https://doi.org/10.1016/j.jeurceramsoc.2018.03.027>
- [9] Kadir Mert Doleker a, Yasin Ozgurluk b , Yasar Kahraman, Oxidation and hot corrosion resistance of HVOF/EB-PVD thermal barrier coating system,2021 <https://doi.org/10.1016/j.surfcoat.2021.126862>
- [10] Hariharan.R , Raja.R, Golden Renjith Nimal R J, Temperature dependence of composition in Ta-Zr-N thin film Deposited by Magnetron Sputtering, Advancement in Engineering, Science & Technology J. Mech. Cont.& Math. Sci., Special Issue, No.-2, August (2019) pp 680-688.
- [11] R.Hariharan, R.Raja, Somu.Vasu, Mechanical and tribological behaviour of thin TaN coating produced on AISI 1018 substrate by DC magnetron sputtering, Volume-7 Issue-6S2, April 2019,IJRTE.
- [12] L.E. Koutsokeras, G. Abadias, Ch.E. Lekka, G.M. Matenoglou, D.F. Anagnostopoulos, G.A. Evangelakis, P. Patsalas, Appl Phys Lett. 93 (2008) 011904.